

Effects of boron addition to the atomic structure and soft magnetic properties of FeCoB films

Aria Yang,^{1,a)} Hassan Imrane,¹ Jing Lou,¹ Johnny Kirkland,² Carmine Vittoria,¹ Nian Sun,¹ and Vincent G. Harris¹

¹Center for Microwave Magnetic Materials and Integrated Circuits, Department of Electrical and Computer Engineering, Northeastern University, Boston, Massachusetts 02115, USA

²SFA, Inc., Crofton, Maryland 21114, USA

(Presented on 6 November 2007; received 13 September 2007; accepted 24 November 2007; published online 21 March 2008)

The magnetic, microwave, and the atomic structure properties of $(\text{Fe}_{0.7}\text{Co}_{0.3})_{1-x}\text{B}_x$ sputtered films on glass substrates were investigated. The addition of boron induced a decrease in coercivity and ferromagnetic resonance linewidth. The amorphous structure was formed at $x \sim 0.075$. Extended x-ray absorption fine structure (EXAFS) of Fe and Co showed the reduced Fourier transform (FT) amplitude, and increased Debye-Waller factors as x was increased, indicating the increased disorder due to the thermal and structural displacements. Possible Fe–B bonding was observed with a reduced bond length, which indicates boron atoms' preference for staying in the interstitial sites in bcc unit cell. © 2008 American Institute of Physics. [DOI: 10.1063/1.2838226]

INTRODUCTION

Soft magnetic materials are used in a large variety of electromagnetic devices such as sensors, magnetic recording heads, and integrated inductors, etc. The strong demand of extending the operation frequency range of these devices into the GHz region forces soft magnetic materials to improve their high frequency characteristics.^{1,2} FeCo and FeCoN thin films with Co content in the range of 30–40 at. % have been widely used because of high saturation magnetization.^{3–10} However, because of the large saturation magnetorestriction constant in the range of $(40 \sim 65) \times 10^{-6}$, and a relatively high anisotropy constant K_1 of $\sim 10 \text{ kJ/m}^3$ of FeCo and FeCoN alloys, it is difficult to achieve good softness in these films unless we go to high concentration of Nitrogen which is not suitable.⁷ From this point of view, FeCoB films have attracted extensive attention in recent years because of high saturation magnetization, low coercivity, high anisotropy field, high electric resistivity and high ferromagnetic resonance frequencies which are desired for RF/microwave applications, and also because we can have amorphous films, which eliminate the magnetocrystalline anisotropy.^{11–18}

Here, we investigated the impact of boron addition upon the magnetic, microwave, and structural properties of FeCo alloys. Extended x-ray absorption fine structure (EXAFS) analysis was employed to measure the local atomic properties Fe and Co atoms in these alloy films.

EXPERIMENT

A series of boron-doped FeCo films [i.e., $(\text{Fe}_{70}\text{Co}_{30})_{1-x}\text{B}_x$] were sputter deposited onto glass substrates. Target boron content (x) was varied from 0%–15%. The pressure was maintained at 3 mTorr during the sputter

deposition. The thickness of the films was maintained to less than 50 nm to reduce the self-absorption effects during the EXAFS data collection. $\text{Cu } K\alpha$ θ – 2θ x-ray diffraction (XRD) studies were employed to determine and analyze the long range structure while EXAFS measurements were used to study the short range chemical and structural order. The EXAFS Fe and Co K edge data were collected using the beamline X23B at the National Synchrotron Light Source. The experiments were performed at the room temperature with a fluorescence detector of the Lytle design.¹⁹ The data were refined and fitted to the theoretical standards generated by the FEFF codes²⁰ of Rehr and Albers using the software suite of ATHENA and ARTEMIS²¹ developed by Ravel and Newville. The soft dc magnetic properties were measured using a vibrating sample magnetometer while the microwave magnetic properties measured using ferromagnetic resonance.

RESULTS AND DISCUSSION

X-ray diffraction measurements for the FeCoB samples with x ranges from 0 to 0.09 are shown in Fig. 1(b) and reveal only the body centered cubic phase of the FeCo metal. The lack of evidence for crystalline boride phases suggests that the B atoms occupy interstitial sites or that the boride phase present are below the detection limit of the XRD. In Fig. 1(a), the highest intensity (110) FeCo x-ray diffraction peak position is plotted as a function of B content. The (110) peak position was observed to increase. It is interpreted the d spacing was slowly decreasing as we increased the x from 0 to 0.05. After $x > 0.05$, the FeCo (110) peak 2θ position increased sharply, as the (110) peak widened and amplitude decreased. It indicated that the FeCo films had reduced grain size and may undergo a phase transition from crystalline to amorphous. The XRD measurements revealed a contraction of the lattice with increasing B content. Although such a

^{a)}Electronic mail: fyang@coe.neu.edu.

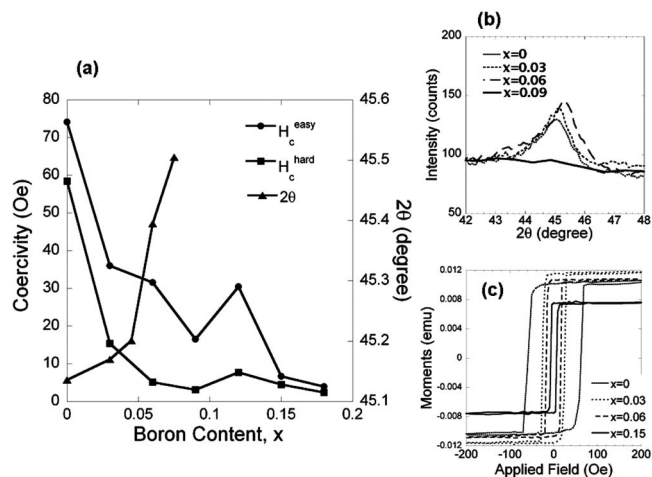


FIG. 1. (a) $\theta-2\theta$ x-ray diffraction FeCo (110) peak position and the coercivity field (measured along easy and hard axes) of the $(\text{Fe}_{70}\text{Co}_{30})_{1-x}\text{B}_x$ films were plotted as a function of boron content x . (b) X-ray diffraction patterns and (c) hysteresis loop along easy axis of the $(\text{Fe}_{70}\text{Co}_{30})_{1-x}\text{B}_x$ films.

trend is counterintuitive, such a contraction has been reported for amorphous alloys marking the transition to a close packed arrangement of atoms.²²

Consequently, the coercivity was measured to decrease proportional to the increasing B content. The coercivity field was also plotted in Fig. 1(a) as a function of x . We measured the hysteresis loop both along the easy and hard axes. The hysteresis loops of those samples with x ranges from 0 to 0.15 along easy axis are shown in Fig. 1(c). The corresponding coercivity values were both plotted showing the same decreasing trend while the coercivity of easy axis hysteresis loop is comparatively larger than the hard axis value. Then phase transition point was around $x=6\%$, which is consistent with the XRD result.

In the ferromagnetic resonance (FMR) measurement, the linewidth was found to decrease from 485 to 29 Oe while the boron content (x) was increased from 0% to 7.5%. This relationship is shown in Fig. 2. The FMR linewidth is the critical factor determining the microwave loss in microwave

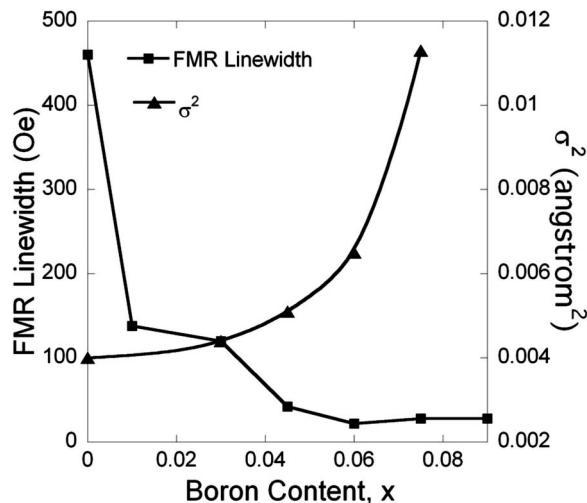


FIG. 2. FMR linewidth and Debye-Waller coefficient as a function of x in the $(\text{Fe}_{70}\text{Co}_{30})_{1-x}\text{B}_x$ films.

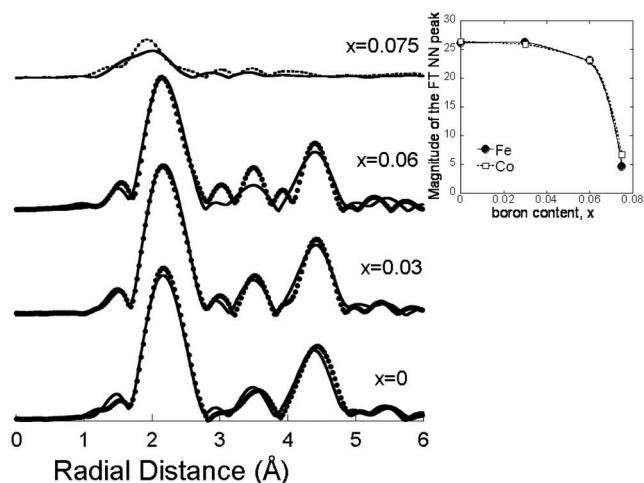


FIG. 3. Fourier transformed Fe and Co K edge EXAFS of the $(\text{Fe}_{70}\text{Co}_{30})_{1-x}\text{B}_x$ films, with different values of x . The solid line represents the Fe K edge data, while the dotted line represents the Co K edge data.

devices. It was obvious from our study that the addition of the boron improves the microwave performance. Also plotted in Fig. 2 is the Debye-Waller coefficient for the first transition metal-transition metal bond determined by our best fit EXAFS model.

EXAFS studies were carried out to better understand the role of boron upon the atomic structure. Following established EXAFS analysis procedures,²³ the extended fine structure data were refined and isolated. It was then converted to photoelectron wave-vector (k) space then Fourier transformed (FT) for the spectral isolation in radial coordinates. The radial positions of the FT peaks represent the distance between the absorbing atom and its near neighbors plus a photoelectron phase shift. The amplitude of the peaks usually indicates the coordination of atoms at those radial distances and their dynamic (thermal) and static atomic disorder. However, in some instances, amplitude from multiple scattering paths also contribute. The FT for both Fe and Co K edge EXAFS data are shown superimposed in Fig. 3. The EXAFS data were refined using a k^3 weighting. Two major peaks appear near $r=2.2$ and 4.4 \AA can be observed in both plots. These peaks represent the unique bonds of the FeCo bcc structure. The FT amplitude of the two peaks was reduced relative to both Fe and Co near neighbors due to the reduction in the chemical order and the introduction of static structural disorder by the presence of the B atom. It is noted that when the boron addition was increased to $x=0.075$, both FT amplitude reduced substantially, with the second peak at around $r=4.4 \text{ \AA}$ vanishing. This indicates that the crystalline ordering has transformed to a largely amorphous phase. Next, we compare the FT data of Fe and Co to extract the local structural information around each atom. The FT EXAFS data for Fe and Co K edges are nearly identical. This suggests that the Fe and Co atoms have common atomic distributions and atomic disorder properties. Since these data have been analyzed using identical refinement procedures, the FT peak amplitudes can be directly compared. As B increases from $x=0$ to 0.06, we measure only small changes in FT amplitude of the order less than 10% with peak amplitude

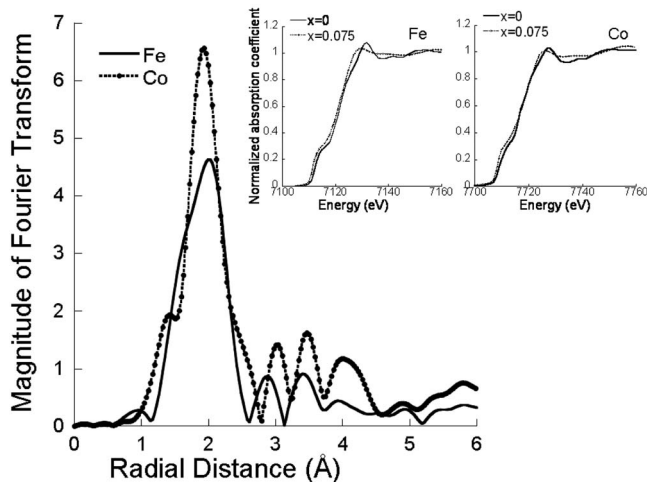


FIG. 4. Fourier transformed EXAFS data for the sample $(\text{Fe}_{70}\text{Co}_{30})_{0.925}\text{B}_{0.075}$. The insets are the x-ray absorption near edge structure (XANES) for Fe and Co K edges. The XANES for $\text{Fe}_{70}\text{Co}_{30}$ was also plotted as a comparison.

reducing as B content increases. However, for $x=7.5\%$, we measure a large reduction of 74% in the FT near neighbor (NN) peak amplitude. The results were included in the Fig. 3. This dramatic transition signals a large increase of the static atomic disorder term corresponding with the evolution of the amorphous structure. It also signals that this evolution is abrupt and does not evolve gradually with B content.

The Fe and Co FT EXAFS and the x-ray absorption near edge structure (XANES) for the sample $(\text{Fe}_{70}\text{Co}_{30})_{0.925}\text{B}_{0.075}$ are plotted in figure 4. In this figure, we observe that the first major FT peak shifts from $r=2.2$ to 1.9 Å for Co, and to 2 Å for Fe. This shift has been reported for other amorphous transition metal systems as a consequence of the amorphous structure. It is also noted that an additional Fourier feature appears near $r=1.5$ Å in the Co FT, and as a pronounced shoulder in the Fe FT figures. We speculate that these features are due to the presence of B residing at the interstitial sites in close proximity to the Fe and Co atoms. Although the feature near the Co atom may be the result of a truncation ripple and residual to the Fourier transformation, the pronounced shoulder on the low- r side of the NN peak in the FT Fe EXAFS is more likely the result of a Fe-B pair correlation. In comparing the Fe to Co FT NN amplitudes, one sees that the Fe has a reduced amplitude due to a greater degree of atomic disorder. This strongly suggests that B resides preferentially near the Fe atom. This affinity is unsurprising due to the stability and strong bonds that form in Fe boride phases. The Fe and Co XANES data presented as an inset to Fig. 4 show very little change between Fe and Co for the $x=0.075$ sample. The changes between the $x=0$ and $x=0.075$ are attributable to the disruption of long range order in the $x=0.075$ sample.

The EXAFS data are capable of providing quantitative information when the FT EXAFS data are fit with theoretical

FEFF standards. The Debye-Waller factor is one of the parameters that can be determined from the EXAFS best fits. This parameter, σ^2 , represents the structural disorder based upon thermal vibrations and static displacements. We have plotted these data in Fig. 2 as a function of x . It clearly increases with increased boron content. In this same figure, we plot the ferromagnetic resonance linewidths. Although there is clearly an inverse relationship between the atomic disorder and both the coercivity and FMR linewidth, it is not monotonic. It is interesting to note that the act of introducing atomic disorder correlates to reduced dc and rf losses. Since this disorder is on the atomic level and much smaller than the exchange volume in this system, these defects do not act to effective pin domain walls. As a result, the materials remain magnetically soft.

ACKNOWLEDGMENTS

This research was performed in part at beamline X23B at the National Synchrotron Light Source at the Brookhaven National Laboratory which is sponsored by the Department of Energy. This research was also supported by the National Science Foundation (DMR 0400676) and the Office of Naval Research (N00014-07-1-0701).

- ¹I. Kim, J. Kim, K. H. Kim, and M. Yamaguchi, *Phys. Status Solidi A* **201**, 1777 (2004).
- ²M. D. Coey, *J. Magn. Magn. Mater.* **226–230**, 2107 (2001).
- ³V. Korenivski and R. B. van Dover, *J. Appl. Phys.* **82**, 5247 (1997).
- ⁴V. Korenivski, *J. Magn. Magn. Mater.* **215–216**, 800 (2000).
- ⁵Y. Jiang, J. Chen, and G. D. Lian, *IEEE Trans. Magn.* **39**, 3559 (2003).
- ⁶C. Kuo, S. S. Chang, C. M. Kuo, Y. D. Yao, and H. L. Huang, *J. Appl. Phys.* **83**, 6643 (1998).
- ⁷X. Sun and S. X. Wang, *IEEE Trans. Magn.* **36**, 2506 (2000).
- ⁸X. Sun, O. F. Xiao, and B. York, *J. Appl. Phys.* **97**, 10F906 (2005).
- ⁹Y. Wang and E. Y. Jiang, *Appl. Phys. A* **A65** 203 (1997).
- ¹⁰K. Seemann, H. Lieste, and V. Bekker, *J. Magn. Magn. Mater.* **283**, 310 (2004).
- ¹¹L. Patt, M. K. Minor, and T. J. Klemmer, *IEEE Trans. Magn.* **37**, 2302 (2001).
- ¹²K. Minor, T. M. Crawford, and T. J. Klemmer, *J. Appl. Phys.* **91**, 8543 (2002).
- ¹³I. Kim, J. Kim, K. H. Kim, and M. Yamaguchi, *IEEE Trans. Magn.* **40**, 2706 (2004).
- ¹⁴M. Munakata, S. I. Aoki, and M. Yagi, *IEEE Trans. Magn.* **41**, 3262 (2005).
- ¹⁵J. Yu, C. Chang, D. Karns, J. Ju, Y. Kubota, W. Eppler, C. Brucker, and D. Weller, *J. Appl. Phys.* **91**, 8357 (2002).
- ¹⁶S. U. Chen, Y. D. Yao, Y. T. Chen, J. M. Wu, C. C. Lee, T. L. Tsai, and Y. C. Chang, *J. Appl. Phys.* **99**, 053701 (2006).
- ¹⁷T. J. Klemmer, K. A. Ellis, L. H. Chen, B. van Dover, and S. Jin, *J. Appl. Phys.* **87**, 830 (2000).
- ¹⁸L. H. Chen, T. J. Klemmer, K. A. Ellis, R. B. van Dover, and S. Jin, *J. Appl. Phys.* **87**, 5858 (2000).
- ¹⁹F. W. Lytle, R. B. Gregor, D. R. Sandstrom, E. C. Marques, J. Wong, C. L. Spiro, G. P. Huffman, and F. E. Huggins, *Nucl. Instrum. Methods Phys. Res. A* **226**, 542 (1984).
- ²⁰J. J. Rehr and R. C. Albers, *Rev. Mod. Phys.* **72**, 621 (2000).
- ²¹B. Ravel and M. Newville, *J. Synchrotron Radiat.* **12**, 537 (2005).
- ²²M. K. Minor, T. M. Craford, T. J. Klemmer, Y. Peng, and D. E. Laughlin, *J. Appl. Phys.* **91**, 8453 (2002).
- ²³D. E. Sayers and B. A. Bunker, in *X-ray Absorption: Principles, Applications, Techniques of EXAFS, SEXAFS and XANES*, edited by D. C. Koningsberger and R. Prins (Wiley, New York, 1988).